Mathematical Geosciences manuscript No.
(will be inserted by the editor)

Optimization of Borehole Thermal Energy Storage Systems Using Genetic Algorithm

Michael Tetteh · Liangping Li · Matthew Minnick · Haiyan Zhou · Zhi Ye

Received: date / Accepted: date

Abstract Borehole Thermal Energy Storage (BTES) represents cutting-edge technology harnessing the Earth's subsurface to store and extract thermal energy for heating and cooling purposes. Achieving optimal performance in BTES systems relies heavily on selecting the right operational parameters. Among these parameters, charging and discharging flow rates play a significant role in determining the amount of heat that can be recovered effectively from the system. In this study, we introduce a Genetic Algorithm as an optimization tool aimed at fine-tuning these operational parameters within a baseline BTES model. The BTES model was developed using FEFLOW and simulated over a 3-year period. After each 3-year simulation, the Genetic Algorithm iteratively adjusted the operational parameters to attain the optimal configuration for maximizing heat recovery from the BTES system. Additional analysis was conducted to explore the impact of BTES system size and borehole spacing on heat recovery. Results indicate that the Genetic Algorithm effectively optimized parameters, leading to enhanced heat recovery efficiency. Moreover, the scenario studies highlighted that closer borehole spacing correlates with higher recovery efficiency.

Keywords Genetic Algorithm · Optimization · Borehole thermal energy storage · Recovery efficiency

Michael Tetteh
Department of Geology and Geological Engineering, South Dakota School of Mines and Technology, Rapid City, 57701, USA

Liangping Li
Department of Geology and Geological Engineering, South Dakota School of Mines and Technology, Rapid City, 57701, USA
E-mail: Liangping.Li@sdsmt.edu

Matthew Minnick
RESPEC Inc., Rapid City, SD 57703, USA

Haiyan Zhou
RESPEC Inc., Rapid City, SD 57703, USA

Zhi Ye
Department of Geology and Geological Engineering, South Dakota School of Mines and Technology, Rapid City, 57701, USA

1 Introduction

Various countries have set targets for achieving net-zero carbon emissions. In the United States, Canada, the UK, and the European Union, a target has been set to achieve net-zero carbon emissions and other greenhouse gases by 2050 (Brown et al. 2023a). However, the dominant role of non-renewable energy such as fossil fuel in meeting the world's energy demands has been a historical constant. Renewable sources of energy are an alternative that will help reduce the growing consumption of fossil fuels. Particularly within the heating sector, excess thermal energy can be temporarily stored and used during peak demand periods (Lanahan and Tabares-Velasco 2017).

Thermal Energy Storage (TES) is a technology that has the ability to store extra energy during times of abundance and release it during peaks in demand (Tamme et al. 2012). This makes it a versatile and scalable solution that improves efficiency and dependability. During times of high energy production or in the summer period, excess heat can be captured by solar collectors, waste heat can be recovered from industrial operations, and heat can be captured from various homes. After being captured, this heat is stored in the subsurface for later use. This thermal energy can be released later to heat homes, especially in the cold seasons, and to power turbines. Thermal energy storage can be performed by exploiting the heat in different ways (Zhang 2016); thermo-chemical storage which utilizes reversible chemical reactions to store and release thermal energy, latent heat storage which stores the energy through phase changes, and sensible heat storage which works by increasing/decreasing the temperature of materials such as water, thermal oils, molten salts, or subsurface geological media.

The subsurface is increasingly being utilized as a reservoir for storing thermal energy, which is referred to as Underground Thermal Energy Storage (UTES) (Aktaş and Kirçiçek 2021). UTES has been exploited in many areas on both large and small scales. Large scale includes commercial and industrial sectors helping to power turbines as well as heating and cooling buildings. It is used on a small scale as a medium to extract heat during the cold season and cold during the hot periods. During the summer, excess heat is stored underground and retrieved in winter for heating, and vice versa for cooling in the summer. This method helps balance seasonal variations in energy demand, contributing to grid stability. UTES uses a variety of storage media (Casasso et al. 2022), including deep aquifers confined by impermeable geological layers for Aquifer Thermal Energy Storage (ATES), and subsurface rock environments accessed through Borehole Heat Exchangers (BHE) for Borehole Thermal Energy Storage (BTES). ATES became popular for storing and retrieving thermal energy both in small and large quantities and also provided a reliable source of thermal energy due to the stable temperature of aquifers (Possemiers et al. 2014). A major setback ATES systems face is unfavorable hydrogeologic conditions (Shi et al. 2023). Not all geological environments possess suitable aquifers for efficient energy storage, making it difficult to store energy through an ATES system. An alternative option to use is a BTES system. BTES is a seasonal storage system that stores heat in soil or rock environment during the summer months through a BHE embedded in the drilled holes to a desired depth. The stored heat is extracted to meet the heating demands in the winter heating season. A BTES system may consist of a single borehole with a coaxial BHE (Xie et al. 2018; Brown et al. 2023b), where fluid is circulated down the annular space, exchanging heat with the subsurface via conduction through the borehole wall before being circulated back to the surface, or an array of boreholes where heat transfer fluid circulates through the BHEs installed in the boreholes to exchange heat with the surrounding rock or sediment mass (Pourahmadiyan et al. 2023). After drilling the boreholes, a U-Tube or coaxial pipe is installed in the borehole, allowing the fluid to continuously circulate from the bottom of the borehole to the surface. Once the piping is fitted, the borehole may be left un-grouted and filled with groundwater, as is common in Scandinavia (e.g., Sweden and Norway) where boreholes are typically drilled in hard rock with the groundwater table a few meters below ground surface (Gehlin 2002), or grout may be poured into the remaining volume of the drilled borehole to provide structural support and improve heat conductivity between the earth and the heat transfer pipes.

While BTES systems offer a sustainable and efficient solution for storing and retrieving thermal energy, one significant area of research is to obtain optimal recovery efficiency (e.g., Wołoszyn 2018; Casasso and Sethi 2014). The ratio of the total thermal energy recovered from the subsurface storage system to the total thermal energy injected during a yearly cycle is known as annual efficiency, which also can be termed as recovery efficiency or round trip efficiency. Therefore, optimizing the BTES system is crucial to achieving optimum energy efficiency. This is important because it reduces operational costs associated with heating and cooling, ensures the long-term sustainability of the BTES system by preventing degradation, wear, and inefficiencies over time, and contributes to the reduction of greenhouse gas emissions by promoting the use of renewable energy sources. For this area of renewable energy where optimization is vital to improve energy efficiency, published work reporting on optimization of the BTES systems is very scanty and optimization has been done mostly by calibration of parameters of the BTES system. For example, Rapantova et al. (2016) utilized a calibrated numerical model (FEFLOW finite element model) to simulate various heat injection and extraction cycles. They conducted calibration using data from six monitoring boreholes, measuring temperatures at depths up to 80 meters underground, with the aim of minimizing heat loss through dissipation to the ground. Kumawat et al. (2024) conducted sensitivity studies to evaluate BTES system performance across a range of operational, design, and geological parameters. Fiorentini and Baldini (2021) focused on operational optimization within a framework designed to identify optimal operating conditions for heat pump-driven BTES systems under different electricity CO_2 intensity profiles. Their work introduced a novel linearized control-oriented model describing storage temperature dynamics under varying operational scenarios. Zhu et al. (2019) explored relationships between input parameters and output indicators through global sensitivity analysis coupled with 3D transient numerical methods, revealing significant interactions among different input variables influencing BTES performance. Disadvantages of manual calibration are the time cost of obtaining the optimal parameters used in the design of the BTES system and the uncertainty that the achieved optimum recovery of heat after manual calibration is indeed the true recovery capacity of a particular BTES system.

In order to successfully navigate the complexity involved in improving BTES systems, integration of modern optimization techniques is essential. Metaheuristic algorithms have been introduced previously to find optimal and near-optimal solutions for complex optimization problems. One optimzation algorithm that falls under the umbrella of the metaheuristic algorithms is particle swarm optimization (PSO), introduced by Kennedy and Eberhart (1995) drawing inspiration from the collective behavior of birds and fish. PSO involves three main controlling parameters—inertia weight, cognitive ratio, and social ratio—where even a slight adjustment can lead to different performances, as demonstrated by Eltamaly et al. (2020) and Harrison et al. (2018). PSO also has some limitations; with regard to complex and large datasets, it produces poor results. When faced with a considerable number of dimensions in the given problem, PSO often struggles to identify the global optimum solution. This issue arises not only from the entrapment in local optima but also from the potential variation in particle velocities, restricting the successive range of attempts to a subset of the overall search space (Pant et al. 2009; Gad 2022).

Another type of metaheuristic algorithm is simulated annealing (SA). It stands out as a versatile and potent optimization technique, particularly adept at identifying global optima amidst numerous local optima. The term "annealing" draws an analogy from thermodynamics, specifically the cooling and annealing process observed in metals (Press and Teukolsky 1991). In simulated annealing, the optimization problem's objective function is employed, instead of using material energy in the metallurgical context. SA is recognized as a straightforward yet highly effective metaheuristic approach in solving global optima problems, especially where the objective function is not explicitly defined and can only be assessed through computationally intensive simulations (Delahaye et al. 2019).

Genetic Algorithm (GA) (Holland 1975) is another type of metaheuristic algorithms that emerged as a cutting-edge methodology to navigate the complexity inherent in optimizing BTES systems. It stands as one of the oldest and most widely recognized optimization techniques inspired by natural processes. Within the framework of GA, the exploration of solution space mimics the natural occurrences observed in the environment, incorporating principles from Darwinian theory of species evolution (Slowik and Kwasnicka 2020). GAs offer several advantages over conventional optimization methods, with two particularly noteworthy strengths: their capability to handle complex problems and their inherent parallelism (Yang 2021). GAs exhibit versatility in addressing diverse optimization types, accommodating objective functions that are either stationary or non-stationary (changing over time), linear or nonlinear, continuous or discontinuous, and those affected by random noise. The parallelism inherent in genetic algorithms stems from multiple offspring within a population acting as independent agents, enabling the exploration of the search space in numerous directions simultaneously. GAs employ three key operators during the optimization process: selection, crossover, and mutation. The selection process involves selecting the best individuals from the current generations as parents to form a mating pool for producing offspring for the next generation. Individuals are selected based on their fitness, which is determined by their performance with respect to the objective function. Individuals with higher fitness are selected to form the mating pool. selection mimics the natural selection process, where individuals with better adaptability are more likely to pass their genetic information to the next generation. After forming the mating pool, a crossover operation is implemented. Crossover involves combining genetic information from two parents to produce offspring with a mix of their traits, thereby exploring new regions of the solution space. Parts of the genetic information (chromosomes) from two parents are exchanged, creating one or more offspring. Common methods include one-point crossover, two-point crossover, and uniform crossover. Crossover introduces diversity in the population, allowing the algorithm to exploit the beneficial combinations of traits present in the parent individuals. Mutation introduces random changes in the genetic information of individuals, preventing the algorithm from getting stuck in local optima and promoting exploration of the search space. A percentage of genes in an individual's chromosome is randomly changed. The percentage is generally termed as mutation rate which determines the likelihood of a gene being mutated.

Optimizing a BTES system entails addressing numerous parameters, including borehole spacing, operational parameters such as the flow rates, design parameters such as the thermal conductivity of the grouting material, and other factors. The challenge lies in finding a configuration that maximizes energy storage and recovery, minimizes losses, and adapts to varying thermal demands. GA excel in tackling such multidimensional optimization problems, offering a holistic approach to fine-tuning the intricate parameters of BTES systems. In this study, to be best of our knowledge, GA will be employed for the first time to search for two optimal operational parameters (charging and discharging flow rate) that emerge as critical operating parameters with substantial implications for the performance of a BTES system.

2 Methodology

2.1 Optimization of parameters

In this study, three categories of parameters that influence the recovery efficiency of a BTES system were considered: (a) design, (b) operational, and (c) geological parameters. Design parameters, such as BHE spacing and grout thermal conductivity, influence heat transfer rates, thereby affecting system efficiency. Operational parameters, such as charging and discharging volumetric flow rate, are directly related to energy storage and recovery. Geological parameters consider the thermal conductivity of the ground.

The separation distance between BHEs in a BTES model plays a crucial role in determining the system's effectiveness. If the distance is too small, thermal interference can occur between the boreholes, impacting overall system efficiency. This interference involves the heat transfer fluid from one borehole affecting the surrounding ground of another, diminishing the system's overall effectiveness. Conversely, if the spacing is too large, it can result in increased costs and reduced efficiency. Larger land areas would be needed for the same thermal energy storage, and the heat transfer fluid would have to travel a greater distance, requiring more energy for circulation. Consequently, the optimal spacing between two BHEs in a BTES model must be meticulously considered to optimize the system's performance.

The thermal conductivity of the grout holds significant importance in the context of a BTES model. It dictates the speed at which heat exchange occurs between the ground and the heat transfer fluid circulating within the borehole. Grout is employed to fill the annular space between the borehole wall and the heat exchanger pipes, influencing the heat transfer between the ground and the heat transfer fluid. In cases where the grout exhibits low thermal conductivity, it acts as a thermal barrier, impeding heat transfer and diminishing the efficiency of the BTES system. Conversely, high thermal conductivity in the grout enhances heat transfer, thereby increasing the overall system efficiency. Consequently, the careful selection of a grout material with appropriate thermal conductivity is pivotal for optimizing the performance of a BTES system.

The flow rate during charging and discharging operations emerges as a critical operating parameter with substantial implications for the performance of a BTES system. In the charging phase, the heat transfer fluid circulates through the BTES to store heat in the nearby ground, and the flow rate influences the efficiency of heat transfer from the working fluid to the BTES system. Conversely, in the discharging phase, the heat transfer fluid circulates through the BHEs to release stored heat into a building's heating system. The flow rate during discharging determines the rate at which stored heat is released into a building. While a higher flow rate accelerates heat transfer, impacting the charging and discharging phases, it also could lead to elevated pressure drop, potentially affecting energy consumption and reducing system efficiency. Hence, obtaining an optimal flow rate for both charging and discharging becomes crucial, striking a balance between efficient heat transfer and the energy consumption of the system.

The thermal conductivity of solids determines how easily heat can be transferred between the ground and the wall of the borehole. The rate of heat transfer between the borehole wall and the surrounding geological material is directly influenced by the thermal conductivity of the solid. A geological environment with high thermal conductivity facilitates easier heat transfer compared to an environment with low thermal conductivity. Understanding the thermal properties of the subsurface geologic properties is very crucial for attaining the highest recovery efficiency of the BTES system.

2.2 Finite element model (FEM)

The FEFLOW software (Diersch 2005), which is a finite element modeling tool, was employed to simulate and compute temperature variations in the subsurface while transferring heat during charging and discharging. The temperature changes in the ground around the borehole can be expressed through the following equation:

$$\rho \cdot c \cdot \frac{\partial T}{\partial t} = \nabla \cdot (k \cdot \nabla T) + Q \tag{1}$$

where ρ (kg/m^3) is the density of the ground, c $(J/(kg * K)$ is the specific heat capacity of the ground, and T (^0C) is the temperature, t is time, k $(W/(m * K))$ is the thermal conductivity of the ground, Q (J/s) is the heat source and sink in the system.

The study considered a BTES system with a circular configuration, primarily because of the favorable packing density it provides for boreholes within a designated area. This allows for the efficient installation of more boreholes in a given space, thereby optimizing the overall thermal energy storage capacity of the system (Skarphagen et al. 2019). To streamline our model, we focused on one quadrant of the circular BTES system, as shown in Figure 1.

The FEM model employed is a homogeneous system with a depth of 30 m, consisting of 6 layers with a vertical discretization of 5 m. The modeling of BHEs employs a quasi-stationary computational method based on the work by Eskilson and Claesson (1988). This approach is advantageous for long-term simulations spanning hours or longer, particularly when inflow temperature changes are less frequent and less steep. The quasi-stationary method offers reasonable accuracy at a lower computational cost. The analytical solution assumes local thermal equilibrium between all elements of the BHE (pipes, grout, ground) at any point during the simulation. The model considers a configuration of double U-shaped BHEs connected in parallel. The borehole diameter is 12 cm, with a pipe separation of 4 cm between each U-shaped BHE. The pipes have a diameter of 3.2 cm, and the pipe walls are 0.29 cm thick. Figure 2 shows the cross-section of the borehole heat exchanger. The double U-shaped BHE comprises two pipes with fluid flowing in opposite directions, providing an increased contact area for enhanced heat transfer. The initial temperature of the BTES model before simulation was 10°C. The base case model parameters are listed in table 1 below:

Table 1 BTES model parameters

Parameter	**Value**
Thermal conductivity of solid $(J/m/s/K)$	3
Thermal conductivity of liquid $(J/m/s/K)$	0.65
Volumetric heat capacity of solid $(MJ/m^3/K)$	2.52
Volumetric heat capacity of liquid $(MJ/m^3/K)$	4.2
Grout thermal conductivity $(J/m/s/K)$	3
Inlet pipe thermal conductivity $(J/m/s/K)$	0.42
Outlet pipe thermal conductivity $(J/m/s/K)$	0.42
Inlet temperature during injection (^0C)	45
Inlet temperature during recovery (^0C)	10
Flow rate during charging/discharging $(m^3/day$	20

2.3 Genetic Algorithm

The implementation of the genetic algorithm is demonstrated in the step below. The algorithm goes through a series of generations to obtain optimal results:

Step 1: Generate population:

The initial population consists of random candidate solutions (chromosomes) aimed at optimizing recovery efficiency. Each chromosome represents a potential solution for achieving the highest recovery efficiency. In this context, each chromosome is defined by two real numbers: the first number represents the flow rate during charging, and the second number represents the flow rate during discharging.

Details of Generation:

- Initialization: An initial set of chromosomes was randomly generated.
- Population Size: The population size was set to five, balancing computational complexity with the need for diversity and exploration in the solution space.

$$\mathbf{New}_{pop} = \begin{bmatrix} \mathbf{p}_{1,1} & \mathbf{p}_{1,2} \\ \mathbf{p}_{2,1} & \mathbf{p}_{2,2} \\ \vdots & \vdots \\ \mathbf{p}_{m,1} & \mathbf{p}_{m,2} \end{bmatrix} \tag{2}$$

where p represents the model parameters to be inserted into the FEFLOW model in the fitness function. Each row is a set of parameters also known as chromosomes. p_m represents the m_{th} parameter in the m_{th} chromosome. For this study, the first parameter in each row represents the charging flow rate and the second parameter is the discharging flow rate.

Step 2: Compute the fitness function:

$$Fitness\ \ function = f(\mathbf{New_{pop}}) \tag{3}$$

where $f(.)$ represents the fitness function. In the fitness function, each chromosome is first inserted into the FEFLOW model. Subsequently, following the model's execution, we calculate the recovery efficiency, $RE = \frac{\nabla H_{recovered}}{\nabla H_{stored}} \times 100\%$ as our objective function. The objective is to maximize this function, which is the RE.

Step 3: Selection of parents:

In this step, parents (chromosomes) are selected based on their fitness scores to ensure that superior solutions have a higher likelihood of passing their genetic material to the next generation. Consequently, in this step, the chromosome with the lowest RE is excluded, while the remaining chromosomes are retained as parents to generate offspring for the next generation.

Selection Method: The tournament selection method was employed for this selection process. This method involves randomly choosing a subset (tournament size) of chromosomes from the population and selecting the fittest chromosome from this subset as a parent. Tournament selection provides a balanced approach that is robust to noise and outliers in fitness values.

Process:

- Randomly select a fixed number of chromosomes (tournament size) from the population.
- Evaluate their fitness and select the chromosome with the highest fitness as a parent.
- Repeat the process to select multiple parents for crossover.

$$\mathbf{Parent} = \begin{bmatrix} \mathbf{p}_{1,1} & \mathbf{p}_{1,2} \\ \mathbf{p}_{2,1} & \mathbf{p}_{2,2} \\ \vdots & \vdots \\ \mathbf{p}_{m-1,1} & \mathbf{p}_{m-1,2} \end{bmatrix} \tag{4}$$

Step 4: Crossover function:

After selecting the parents, the chromosome with the highest RE replaces the eliminated chromosome to maintain the original size of the population. Subsequently, the crossover function is employed to merge two chromosomes, exchanging portions of parameters between them. The population generated after the crossover function is termed the offspring.

Process:

Crossover Points: In this case, a single-point crossover was employed because the chromosome contains only two values, making the crossover point the last value in the chromosome.

Offspring Creation: Apply crossover to pairs of selected parent chromosomes to generate offspring that inherit genetic information from both parents.

$$\mathbf{Offspring} = \begin{bmatrix} \mathbf{p}^*_{1,1} & \mathbf{p}^*_{1,2} \\ \mathbf{p}^*_{2,1} & \mathbf{p}^*_{2,2} \\ \vdots & \vdots \\ \mathbf{p}^*_{m,1} & \mathbf{p}^*_{m,2} \end{bmatrix} \tag{5}$$

Step 5: Mutation:

In the final stages of the genetic algorithm's implementation, the mutation step is applied. During this step, all chromosomes are selected for mutation. Genes within each chromosome are chosen randomly, ensuring that each gene has an equal chance of being mutated.

3 Synthetic Cases

In this study, a genetic algorithm is employed to optimize the two operational parameters, while the grout thermal conductivity and the thermal conductivity of the ground remains fixed. This study considered two BHE spacings, a 2.5 m spacing and a 10 m spacing. The genetic algorithm ran for 30 generations because, following a pilot experiment, there was a considerable reduction in recovery efficiency differences from the 25th generation to the 30th generation. The objective was to explore the efficacy of mathematical algorithms in obtaining optimal parameters for a BTES system design. Algorithm 1 shows the process of implementing the optimization. During the optimization process, three scenarios were considered, as shown in Table 2. These scenarios are presented to analyze the impact of the number of boreholes and their spacing on the overall heat recovery efficiency. The implementation of the genetic algorithm for the optimization process is illustrated in algorithm 1.

Table 2 Scenarios studies.

Scenarios	BHE spacing (m)	Number of BHEs
1	2.5	127
2	2.5	37
3	10	13

Algorithm 1: Optimization of Parameters using Genetic Algorithm and FEFLOW Model

```
Set: N_w = Number of parameters
Set: N_pop = Number of population
Set: N_gen = Number of generations
begin
    Generate new population, New_pop = (N_pop, N_w)
    for generation = 1, 2, ··· , N_gen do
        Implement the fitness function
        for i = 1, 2, ··· , N_pop do
            Insert parameters into the FEFLOW model
            Run Feflow model and calculate recovery efficiency (RE)
            RE = ∇H_recovered / ∇H_stored × 100%
        Select the best chromosomes in the current population to join the mating pool:
        for i = 1, 2, ··· , N_pop do
            Eliminate the chromosome with the least RE
        Replace it with the chromosome with the highest RE
        parent = (N_pop, N_w)
        Generate next generation using the crossover function:
        offspring = (N_pop, N_w)
        Add variation to the offspring using the mutation function:
        New_pop = (N_pop, N_w)
end
```

4 Results

4.0.1 Optimization for 2.5 m BHE spacing

The optimization process for the BTES with a 2.5 m BHE spacing considered two scenarios. In the first scenario, a large number of BHEs, approximately 127, were deployed, as shown in Figure 3a. The second scenario involved fewer BHEs, approximately 37, as depicted in Figure 3b.

The results of the optimization process for the two scenarios are shown in Figures 4 and 5. For scenario 1, after 30 generations, the optimal recovery efficiency reached approximately 65% by the 28th generation. At this point, the charging and discharging flow rates were approximately 18 m^3/day and 39 m^3/day, respectively. Scenario 2, with fewer BHEs, achieved an approximate recovery efficiency of 52.9% at the 29th generation. The charging and discharging flow rates were approximately 20.5 m^3/day and 36.9 m^3/day, respectively. The results of the analysis provide compelling evidence indicating a direct relationship between the increase in discharging flow rates and the corresponding rise in recovery efficiency. Upon closer examination of Figure 4, a discernible trend emerges wherein successive generations witness a notable uptick in both discharging flow rates and recovery efficiency. This suggests a positive correlation between these variables over time. Additionally, Figure 5 further reinforces this observation by highlighting instances where the algorithm generates higher discharging flow rates, coinciding with significant spikes in recovery efficiency. These findings underscore the importance of monitoring and optimizing discharging flow rates as a critical factor in enhancing overall recovery efficiency within our operational processes. By understanding and leveraging this relationship, we can effectively improve our process performance and achieve greater efficiency.

One of the primary goals of optimizing the recovery efficiency in a BTES system is to maximize the amount of heat recovered from the subsurface while minimizing costs during the design, construction, operation, and production phases of the heat storage and retrieval process. A significant cost factor is the number of wells drilled for the BTES system. More boreholes result in higher initial and maintenance costs. The results of the recovery efficiency after the optimization process for the two scenarios show that using fewer BHEs in scenario 2 (37 BHEs) compared to scenario 1 (127 BHEs) did not result in poor performance. Scenario 2 achieved a RE of 52.9%, despite having less than a third of the boreholes used in scenario 1. Therefore, the optimization process revealed that a substantial reduction in the number of boreholes can still yield significant heat recovery from the BTES system without incurring the additional costs associated with a larger number of boreholes during the design and operation phases.

The analysis also focused on examining the temperature distributions within the BTES model under two different scenarios, as visually represented in Figure 6 and Figure 7. In Scenario 1, characterized by a higher number of 127 BHEs, the temperature distribution appears to be more extensive across the model domain compared to Scenario 2. This disparity arises because Scenario 1 features a greater number of BHEs covering a larger area. Consequently, there are more points within the system where heat exchange occurs, leading to a more even distribution of heat throughout the system. This results in a smoother transition in temperature from the inlet to the outlet, with the temperature change being more gradual and uniform along the length of the BTES system. Conversely, in Scenario 2, which has fewer BHEs covering a smaller area, the distribution of heat exchange points is more limited. As a result, heat transfer becomes more concentrated and localized around these points. This concentration of heat exchange leads to a more abrupt and less gradual temperature change from the inlet to the outlet compared to Scenario 1. Consequently, Scenario 2 exhibits a steeper temperature gradient along the length of the BTES system. Moreover, the higher number of BHEs covering a larger area in Scenario 1 results in a greater density of heat exchange locations per unit area of the model domain. This increased density provides more opportunities for heat exchange to occur across a larger portion of the BTES domain compared to Scenario 2, where fewer BHEs cover a smaller portion of the model domain. Leading to scenario 1 achieving higher recovery efficiency than scenario 2.

Additionally, another contributing factor to the lower temperature levels observed in Scenario 2 could be the migration of a substantial amount of heat to areas devoid of BHEs. This dispersion of heat poses challenges in its retrieval, thereby increasing the likelihood of heat dissipation. Conversely, Scenario 1 benefits from a more extensive coverage of BHEs across a larger portion of the model domain, facilitating more efficient heat retention and retrieval mechanisms. Thus, the interplay between BHE distribution, heat storage capacity, and the dynamics of heat migration in the surrounding environment elucidates the nuanced variations in temperature distributions and the utilization of heat observed between the two scenarios.

4.0.2 Optimization for 10 m BHE spacing

This optimization process involved a 10 m BHE spacing, as illustrated in Figure 8. After 30 generations, the optimal recovery efficiency of approximately 14.9% was achieved in the 30th generation (Figure 9). The charging and discharging flow rates were 24.8 m^3/day and 36.2 m^3/day, respectively. Throughout the process of optimization, there was a little improvement in the overall recovery efficiency. This observation becomes particularly evident upon examining the trends in both charging and discharging flow rates. Across successive generations, there seemed to be minimal changes (increase or decrease) between the previous parameters of charging and discharging flow rates and the subsequent ones generated. However, an interesting pattern emerges when there's a notable difference between the discharging and charging flow rates, specifically when the former exceeds the latter. It is in these instances that a significant increase in recovery efficiency was observed. Moreover, it is worth noting a stark contrast in the flow rate dynamics between this scenario and scenarios 1 and 2. Here, both the charging and discharging flow rates appear to be relatively high. This deviation from the previous scenarios, where the charging flow rates were notably lower compared to discharging flow rates, can be attributed to the larger distances between the BHEs. The greater distance between the BHEs necessitates a higher flow rate to effectively circulate heat through the system and extract it efficiently. Consequently, the requirement for higher flow rates in this scenario highlights the intricate interplay between system design parameters, such as BHE spacing, and operational variables like flow rates, all of which impact the overall efficiency and effectiveness of the system.

Similar to Scenario 1, the cross-section of the model domain reveals a broad temperature distribution. Additionally, the wider spacing between BHEs leads to extensive temperature migration and interaction with surrounding materials, resulting in a decrease in temperature. As depicted in Figure 10, there is a noticeable temperature reduction between successive BHEs. Specifically, the surrounding temperature of the last BHE is approximately 13^oC, which is close to the boundary temperature.

The temperature profile and recovery efficiency for a 3-year cycle are depicted in Figure 11 for both 2.5 m (scenario 1) and 10 m spacings. The analysis reveals distinct trends. During charging, the 10m spacing exhibits a rapid initial temperature rise followed by a gradual increase, while the 2.5 m spacing shows a steady incremental change throughout the charging phase. Throughout the 3-year cycle, the 2.5 m spacing records consistently higher temperatures during the charging phase, with the temperature difference between the two spacings increasing in successive cycles. During discharging, the 2.5 m spacing also records higher temperatures compared to the 10m spacing, with both systems experiencing significant temperature increases in successive cycles, however the 2.5 m spacing scenario recovered more heat than the 10m spacing. These temperature profile trends are reflected in the recovery efficiency, with the 2.5 m spacing consistently achieving higher heat recovery across the 3-year cycle. The difference in recovery efficiency between the two BHE spacings widens at each successive year, indicating that the 2.5 m spacing will continue to recover more heat than the 10m spacing in additional cycles.

4.0.3 Base case vs optimum case

The BTES system for scenario 1 underwent simulation spanning a six-year cycle to conduct a comparative analysis between a base case scenario, characterized by a charging and discharging flow rate of 20 m^3/day, and the optimized configuration of scenario 1. Throughout this simulation, the dynamic interplay between charging and discharging cycles and their consequent impact on outlet temperature variations highlighted the critical importance of optimizing operational parameters for achieving peak system performance.

Figure 12 provides a comparative overview of the recovery efficiency between the base and optimized scenarios. Within the initial year, the base case attained a recovery efficiency of 34.1%, while the optimized scenario showcased a notably higher efficiency of 62.2%. This difference in recovery efficiency signifies that a larger proportion of the energy injected is recovered during the discharging phase in the optimized scenario, thereby enhancing the energy efficiency and cost-effectiveness of the BTES system. Furthermore, it also implies a diminished environmental footprint, as the system operates with greater efficiency, thereby minimizing energy wastage.

To comprehensively evaluate the long-term efficacy of the BTES system, it's imperative to consider the recovery rates across multiple cycles. Over the span of the six-year cycle, the base case peaked at a recovery efficiency of 60.6%, whereas the optimized scenario consistently outperformed, achieving a significantly higher recovery efficiency of 96.5%. The widening gap in recovery efficiency between the optimized and base scenarios with each successive cycle underscores the optimized scenario's ability to extract more heat per cycle compared to the base scenario, indicating sustained superior performance over time.

5 Discussion

Several sensitivity analysis studies have been conducted to determine the impact of design, operational, and geological parameters on BTES system efficiency. These studies focus on optimizing the heat transfer process, minimizing heat loss, and enhancing overall system performance. Han and Yu (2016) conducted a sensitivity analysis on geological attributes (initial ground temperature, groundwater velocity, and thermal properties of materials), design factors (borehole depth), and operational parameters (working fluid velocity, inlet temperature, and intermittent mode) for a vertical Ground Source Heat Pump (GSHP). The results showed that geological properties, borehole depth, and working fluid velocity significantly influence performance, while specific heat capacity showed no noticeable impact. Wołoszyn and Gołaś (2014) analyzed BTES efficiency with single U-tube boreholes, focusing on geological thermal properties, including thermal conductivity, specific heat, and density of the rock mass and grout material. The study found that thermal conductivity of the rock mass had the most significant impact. Wołoszyn (2018) conducted a global sensitivity analysis (GSA) on BTES efficiency during long-term operation, assessing the influence of BHE arrangement parameters (distance between BHE axes in the x-direction and y-direction, and the angle between the top surface of the rock mass and borehole axes). The results showed that BHE inclination crucially impacts BTES efficiency. Baser and McCartney (2015) studied the influence of different variables on a BTES model with five boreholes, including heat injection rate, duration, ground thermal conductivity, and borehole spacing. The study indicated that soil with lower thermal conductivity had less lateral heat loss, and arrays with smaller borehole spacing allowed more concentrated heat storage at higher temperatures. Kumawat et al. (2024) conducted a sensitivity analysis of BTES modeling on a wedge-shaped model, examining five parameters: well spacing, grout thermal conductivity, charging and discharging rates, and soil thermal conductivity. The analysis revealed that BHE spacing and volumetric flow rate had the highest impact on roundtrip efficiency.

Other optimization techniques for BTES systems have also been studied. Schulte et al. (2015) presented an approach for simulating and optimizing borehole thermal energy storage systems, using a software tool to optimize the number and length of borehole heat exchangers based on specific annual heat demand. The tool effectively determined the ideal size of the thermal energy storage, showing that BTES systems operate efficiently in large-scale applications. Fiorentini and Baldini (2021) proposed a control-oriented numerical optimization model to determine the best operating conditions for a heat pump-driven BTES, aiming to reduce yearly CO_2 emissions by shifting the heat pump's electricity load based on CO_2 intensity profiles. The study demonstrated that this boundary condition is crucial for optimal system operation. Rapantova et al. (2016) optimized the lengths of charging and discharging cycles to minimize heat loss due to ground dissipation, finding borehole depth optimization crucial for reducing heat exchange surface area and heat losses. Lanini et al. (2014) established a 1D analytical model and a 3D multilayer numerical model, validated against experimental data, to simulate different configurations over many years. The study included a full-scale experiment evaluating the energetic potential of BTES, showing that the heat transfer fluid lost 15% of its energy at a depth of 100 m and 25% at 150 m.

The conclusions from these studies primarily analyze the influence of various BTES parameters on system performance. While geological parameters (e.g., ground thermal conductivity) significantly affect performance, they cannot be easily altered to optimize heat recovery. However, operational and design parameters, as noted in the literature, also have a significant influence and can be regulated for optimal recovery. Existing theoretical research on optimizing BTES parameters for optimal heat recovery is insufficient. In this paper, we propose a method using a genetic algorithm to optimize BTES recovery efficiency by automatically adjusting the operational parameters (charging and discharging flow rate) of the BTES system. The results were promising, indicating that by using the genetic algorithm to calibrate the BTES operational parameters, and adjusting the BHE spacing, optimal recovery efficiency was achieved after the optimization process.

6 Conclusion

This research study aimed to optimize the operation of BTES systems by utilizing a genetic algorithm to compute optimal parameters for maximizing energy recovery. The study focused on design, operational, and geological parameters. Design parameters included thermal conductivity of the grout and BHE spacing, with two spacing configurations considered. The geological parameter was the subsurface's thermal conductivity, of which both the subsurface's thermal conductivity and the grout thermal conductivity were held constant. The optimization algorithm focused on operational parameters, such as charging and discharging flow rates. Finite element simulation was employed to simulate the BTES system and compute recovery efficiency as the performance metric for testing the optimized parameters.

The results highlighted the intricate relationship between recovery efficiency, BHE spacing, and the volumetric charging and discharging flow rates within the BTES system. It was evident that smaller BHE spacing correlated with higher recovery rates, while, within a specific BHE spacing, higher discharging flow rates contributed to enhanced recovery efficiency. However, an interesting observation emerged regarding the interplay between BHE spacing and flow rates during charging. It was noted that when the BHE spacing was smaller, the flow rate during charging tended to be lower compared to configurations with larger BHE spacing. This suggests a trade-off between BHE spacing and flow rates during charging, indicating the need for careful consideration when optimizing these parameters. Moreover, an optimal BTES model was developed and compared against the base case. The findings revealed that the optimal model achieved an impressive recovery efficiency of 96.5% over a simulated six-year period. This highlights the effectiveness of optimizing system parameters in maximizing energy recovery and overall system performance.

By delving into the impact of various parameters on system performance, this study contributes to the use of mathematical algorithms for obtaining optimal parameters, ultimately enhancing the efficient design and operation of BTES systems.

Acknowledgements. This work has been supported through a grant from the National Science Foundation (OIA-1833069). The authors wish to thank two anonymous reviewers for their comments, which substantially helped to improve the final version of the manuscript.

References

Aktaş, A., Kirçiçek, Y., 2021. Chapter 6 - solar thermal systems and thermal storage, in: Aktaş, A., Kirçiçek, Y. (Eds.), Solar Hybrid Systems. Academic Press, pp. 127–137.

Baser, T., McCartney, J.S., 2015. Development of a full-scale soil-borehole thermal energy storage system, pp. 1608–1617.

Brown, C.S., Desguers, T., Lyden, A., Kolo, I., Friedrich, D., Falcone, G., 2023a. Modelling Borehole Thermal Energy Storage using Curtailed Wind Energy as a Fluctuating Source of Charge , 6–8.

Brown, C.S., Doran, H., Kolo, I., Banks, D., Falcone, G., 2023b. Investigating the influence of groundwater flow and charge cycle duration on deep borehole heat exchangers for heat extraction and borehole thermal energy storage. Energies 16. doi:10.3390/en16062677.

Casasso, A., Giordano, N., Bianco, C., Sethi, R., 2022. Utes - underground thermal energy storage, in: Cabeza, L.F. (Ed.), Encyclopedia of Energy Storage. Elsevier, Oxford, pp. 382–393.

Casasso, A., Sethi, R., 2014. Sensitivity analysis on the performance of a ground source heat pump equipped with a double u-pipe borehole heat exchanger. Energy Procedia 59, 301–308. European Geosciences Union General Assembly 2014, EGU Division Energy, Resources & the Environment (ERE).

Delahaye, D., Chaimatanan, S., Mongeau, M., 2019. Simulated annealing: From basics to applications, in: Gendreau, M., Potvin, J.Y. (Eds.), Handbook of Metaheuristics. Springer. volume 272 of *International Series in Operations Research & Management Science (ISOR)*, pp. 1–35.ISBN 978–3–319–91085–7.

Diersch, H.J., 2005. FEFLOW Software—Finite Element Subsurface Flow and Transport Simulation System—Reference Manual.

Eltamaly, A.M., Al-Saud, M., Abokhalil, A.G., Farh, H.M., 2020. Simulation and experimental validation of fast adaptive particle swarm optimization strategy for photovoltaic global peak tracker under dynamic partial shading. Renewable and Sustainable Energy Reviews 124, 109719.

Eskilson, P., Claesson, J., 1988. Simulation model for thermally interacting heat extraction boreholes. Numerical heat transfer 13, 149–165.

Fiorentini, M., Baldini, L., 2021. Control-oriented modelling and operational optimization of a borehole thermal energy storage. Applied Thermal Engineering 199, 117518.

Gad, A.G., 2022. Particle swarm optimization algorithm and its applications: A systematic review. Archives of Computational Methods in Engineering 29, 2531–2581.

Gehlin, S., 2002. Thermal response test: method development and evaluation. Master's thesis. Luleå tekniska universitet.

Han, C., Yu, X.B., 2016. Sensitivity analysis of a vertical geothermal heat pump system. Applied Energy 170, 148–160.

Harrison, K.R., Engelbrecht, A.P., Ombuki-Berman, B.M., 2018. Optimal parameter regions and the time-dependence of control parameter values for the particle swarm optimization algorithm. Swarm and Evolutionary Computation 41, 20–35.

Holland, J., 1975. Adaptation in Natural and Artificial Systems. University of Michigan Press, Ann Arbor. 2nd Edition, MIT Press, 1992. .

Kennedy, J., Eberhart, R., 1995. Particle swarm optimization, in: Proceedings of ICNN'95 - International Conference on Neural Networks, pp. 1942–1948 vol.4.

Kumawat, P.K., Zhou, H., Kitz, K., McLennan, J., Powell, K., Deo, M., Panja, P., 2024. Sensitivity analysis of borehole thermal energy storage (btes): Examining key factors for system optimization. Energy Storage and Saving .

Lanahan, M., Tabares-Velasco, P.C., 2017. Seasonal thermal-energy storage: A critical review on btes systems, modeling, and system design for higher system efficiency. Energies 10.

Lanini, S., Delaleux, F., Py, X., R.Olivès, Nguyen, D., 2014. Improvement of borehole thermal energy storage design based on experimental and modelling results. Energy and Buildings 77, 393–400.

Pant, M., Thangaraj, R., Abraham, A., 2009. Particle Swarm Optimization: Performance Tuning and Empirical Analysis. Springer Berlin Heidelberg, Berlin, Heidelberg. pp. 101–128.

Possemiers, M., Huysmans, M., Batelaan, O., 2014. Influence of aquifer thermal energy storage on groundwater quality: A review illustrated by seven case studies from belgium. Journal of Hydrology: Regional Studies 2, 20–34.

Pourahmadiyan, A., Sadi, M., Arabkoohsar, A., 2023. 6 - seasonal thermal energy storage, in: Arabkoohsar, A. (Ed.), Future Grid-Scale Energy Storage Solutions. Academic Press, pp. 215–267.

Press, W.H., Teukolsky, S.A., 1991. Simulated Annealing Optimization over Continuous Spaces. Computer in Physics 5, 426–429.

Rapantova, N., Pospisil, P., Koziorek, J., Vojcinak, P., Grycz, D., Rozehnal, Z., 2016. Optimisation of experimental operation of borehole thermal energy storage. Applied Energy 181, 464–476.

Schulte, D.O., Rühaak, D.W., Oladyshkin, D.S., Welsch, B., Sass, P.I., 2015. Optimization of medium-deep borehole thermal energy storage systems. Energy Technology 4.

Shi, Y., Cui, Q., Song, X., Liu, S., Yang, Z., Peng, J., Wang, L., Guo, Y., 2023. Thermal performance of the aquifer thermal energy storage system considering vertical heat losses through aquitards. Renewable Energy 207, 447–460.

Skarphagen, H., Banks, D., Frengstad, B.S., Gether, H., 2019. Design considerations for borehole thermal energy storage (btes): A review with emphasis on convective heat transfer. Geofluids doi:https://doi.org/10.1155/2019/4961781.

Slowik, A., Kwasnicka, H., 2020. Evolutionary algorithms and their applications to engineering problems. Neural Computing and Applications 32, 12363–12379.

Tamme, R., Laing, D., Steinmann, W.D., Bauer, T., 2012. Thermal Energy Storagethermalenergy storage. Springer New York, New York, NY. pp. 10551–10577.

Wołoszyn, J., 2018. Global sensitivity analysis of borehole thermal energy storage efficiency on the heat exchanger arrangement. Energy Conversion and Management 166, 106–119.

Wołoszyn, J., Gołaś, A., 2014. Sensitivity analysis of efficiency thermal energy storage on selected rock mass and grout parameters using design of experiment method. Energy Conversion and Management 87, 1297–1304.

Xie, K., Nian, Y.L., Cheng, W.L., 2018. Analysis and optimization of underground thermal energy storage using depleted oil wells. Energy 163, 1006–1016.

Yang, X.S., 2021. Chapter 6 - genetic algorithms, in: Yang, X.S. (Ed.), Nature-Inspired Optimization Algorithms (Second Edition). second edition ed.. Academic Press, pp. 91–100.

Zhang, Y., 2016. Research of thermal energy storage technology in the solar thermodynamic power. Journal of Power and Energy Engineering 4, 42–49.

Zhu, L., Chen, S., Yang, Y., Tian, W., Sun, Y., Lyu, M., 2019. Global sensitivity analysis on borehole thermal energy storage performances under intermittent operation mode in the first charging phase. Renewable Energy 143, 183–198.

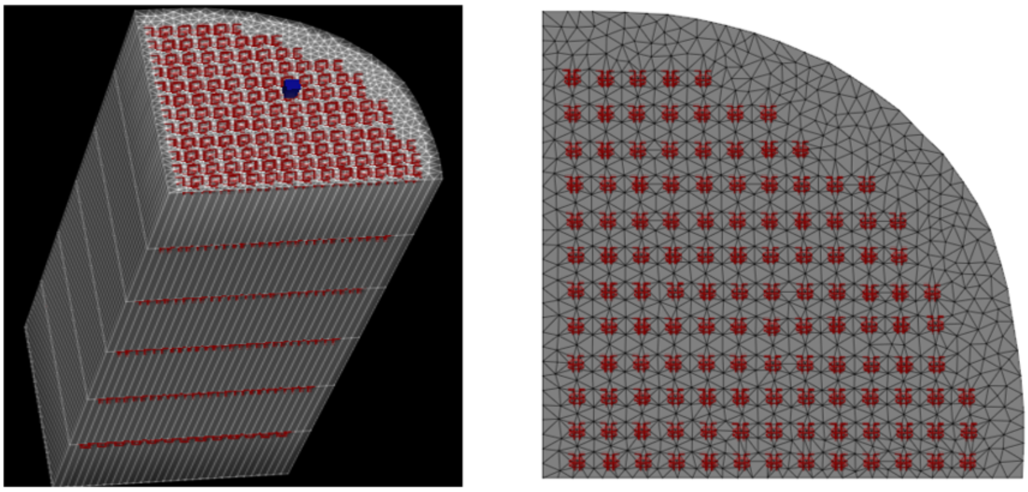

Fig. 1 Finite element model grid for this study

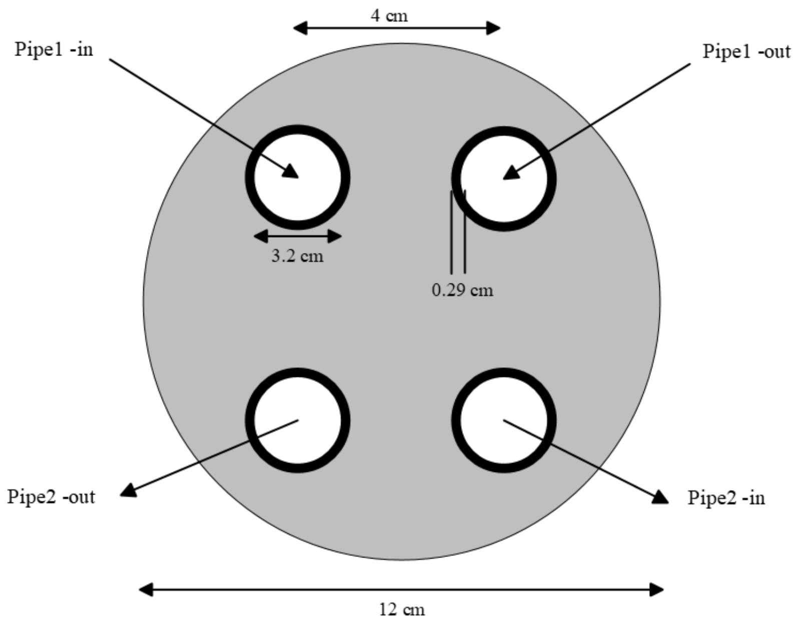

Fig. 2 Cross-section of the borehole heat exchanger

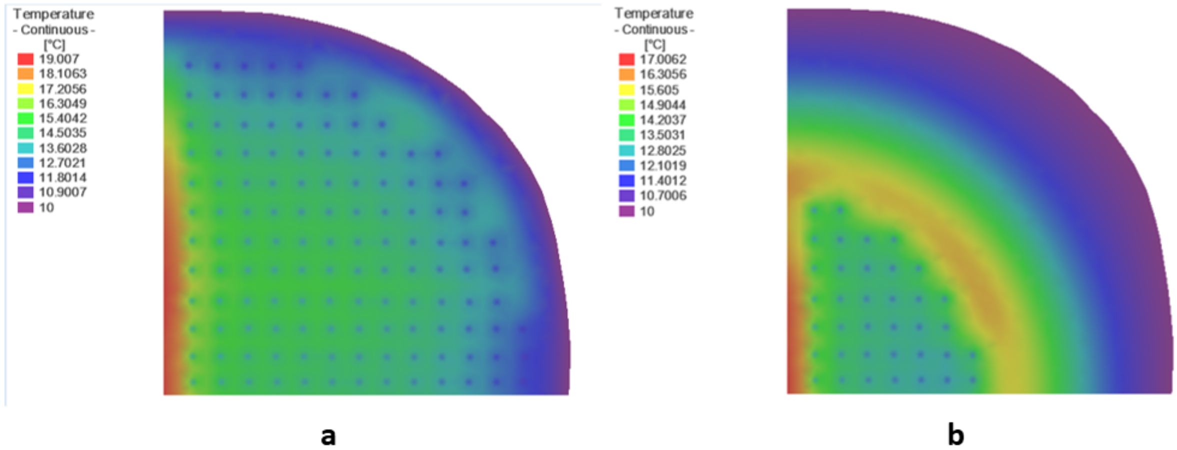

Fig. 3 Top view of a simulated BTES system containing: a. 127 BHEs and b. 37 BHEs

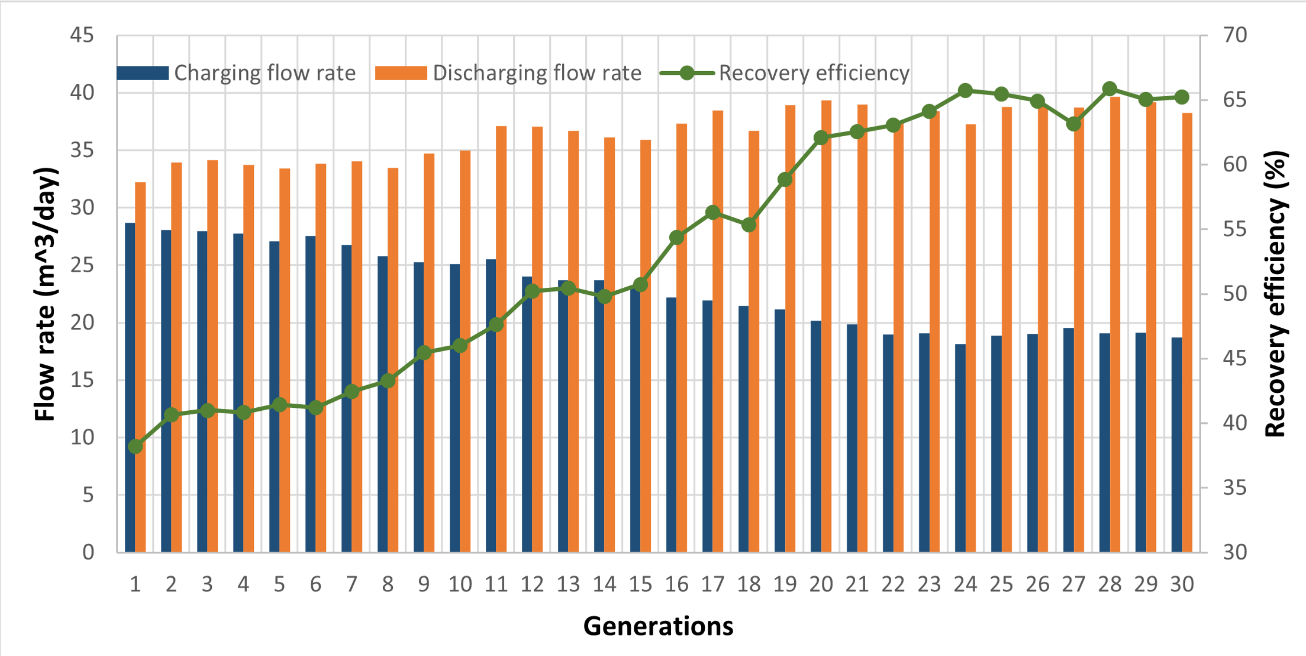

Fig. 4 Optimal parameters and recovery efficiency for scenario 1

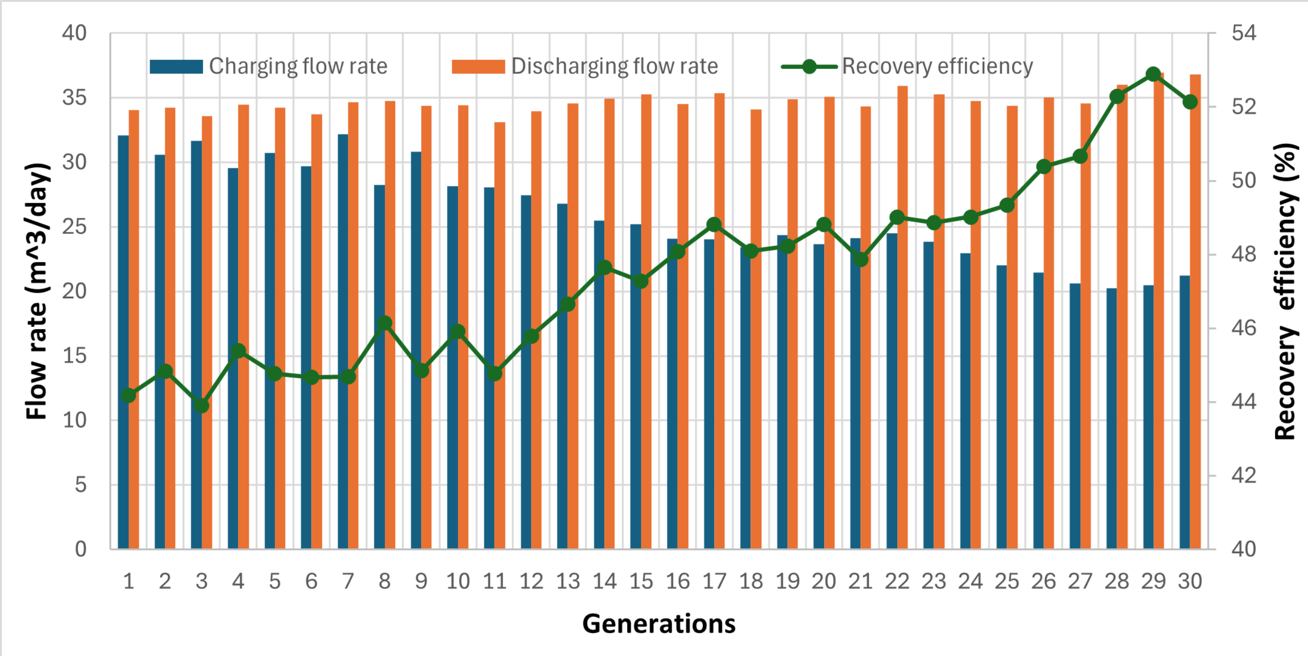

Fig. 5 Optimal parameters and recovery efficiency for scenario 2

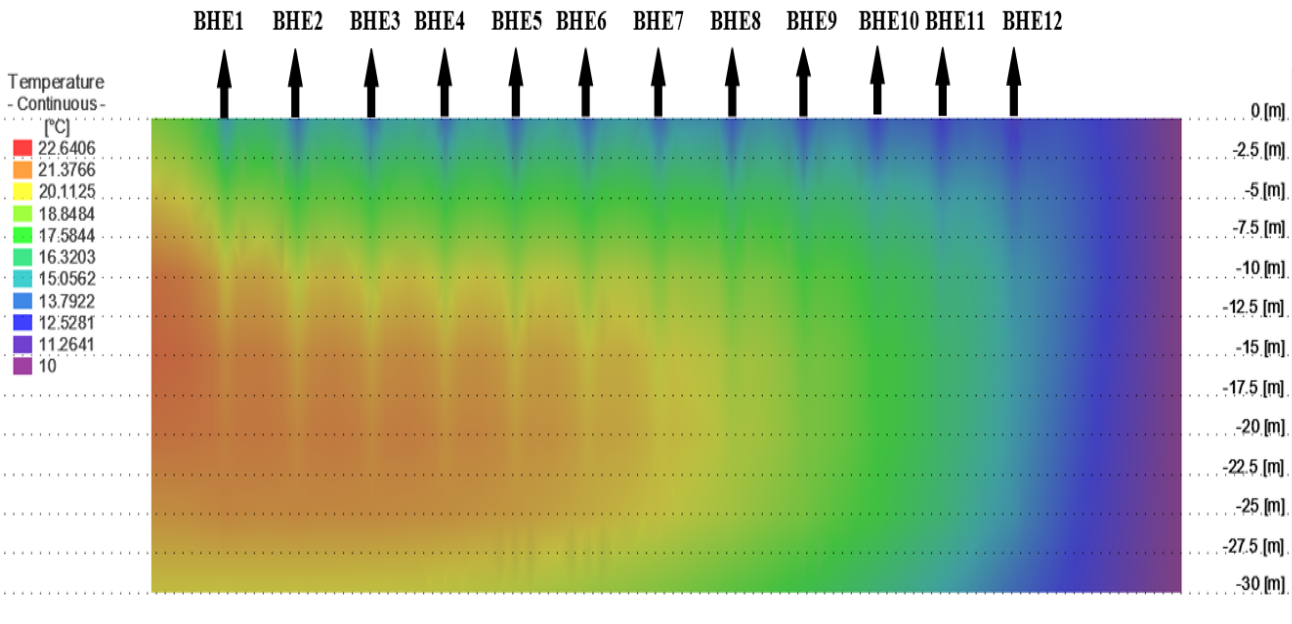

Fig. 6 Cross-section of the BTES model showing spatial distribution of temperature after 3-year cycle for scenario 1

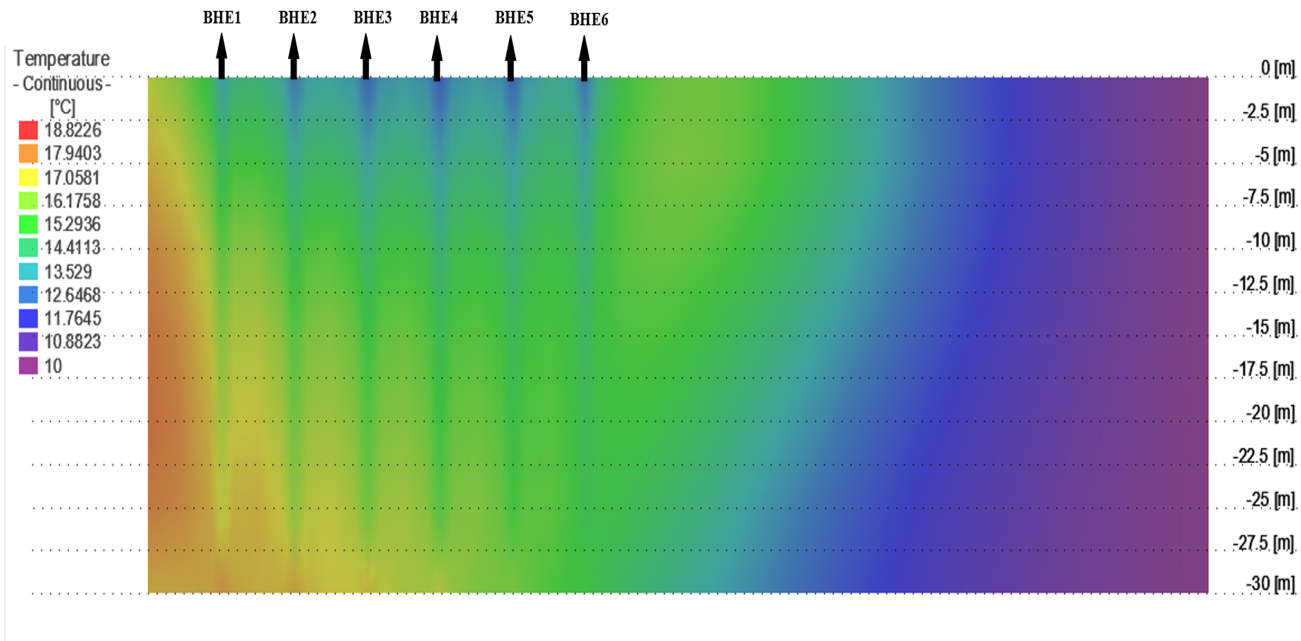

Fig. 7 Cross-section of the BTES model showing spatial distribution of temperature after 3-year cycle for scenario 2

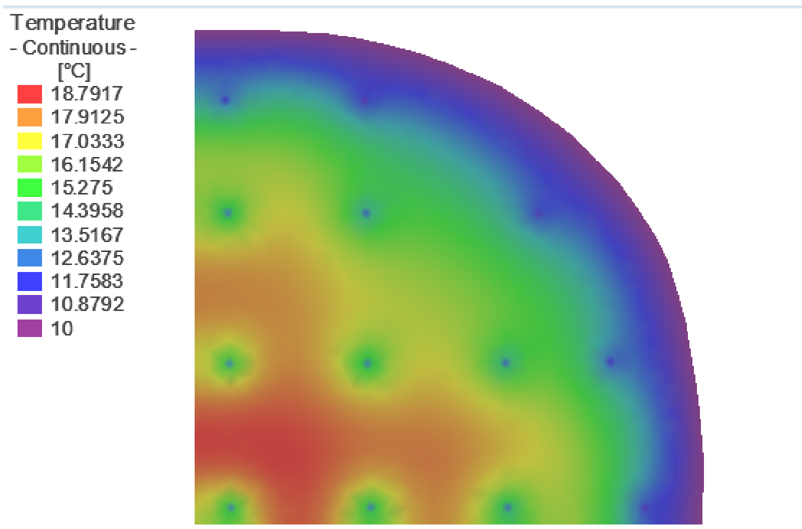

Fig. 8 Top view of the simulated BTES system for 10m BHE spacing

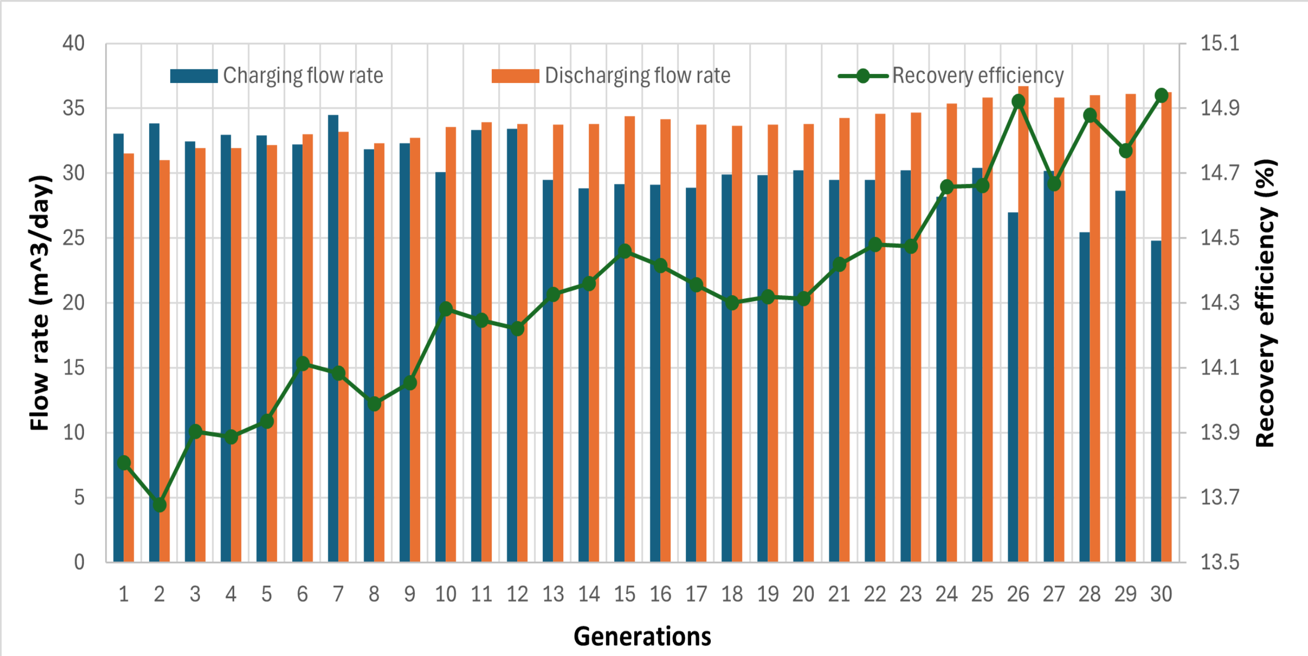

Fig. 9 Optimum parameters and recovery efficiency for scenario 3

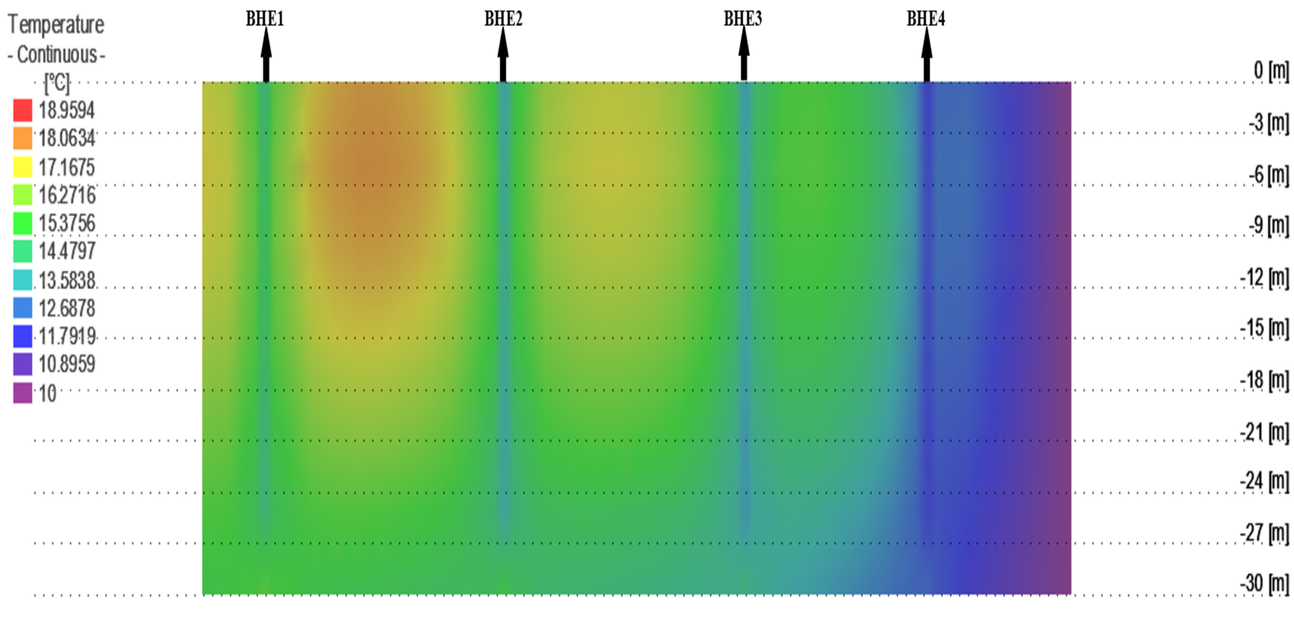

Fig. 10 Cross-section of the BTES model showing spatial distribution of temperature after 3-year cycle for scenario 3

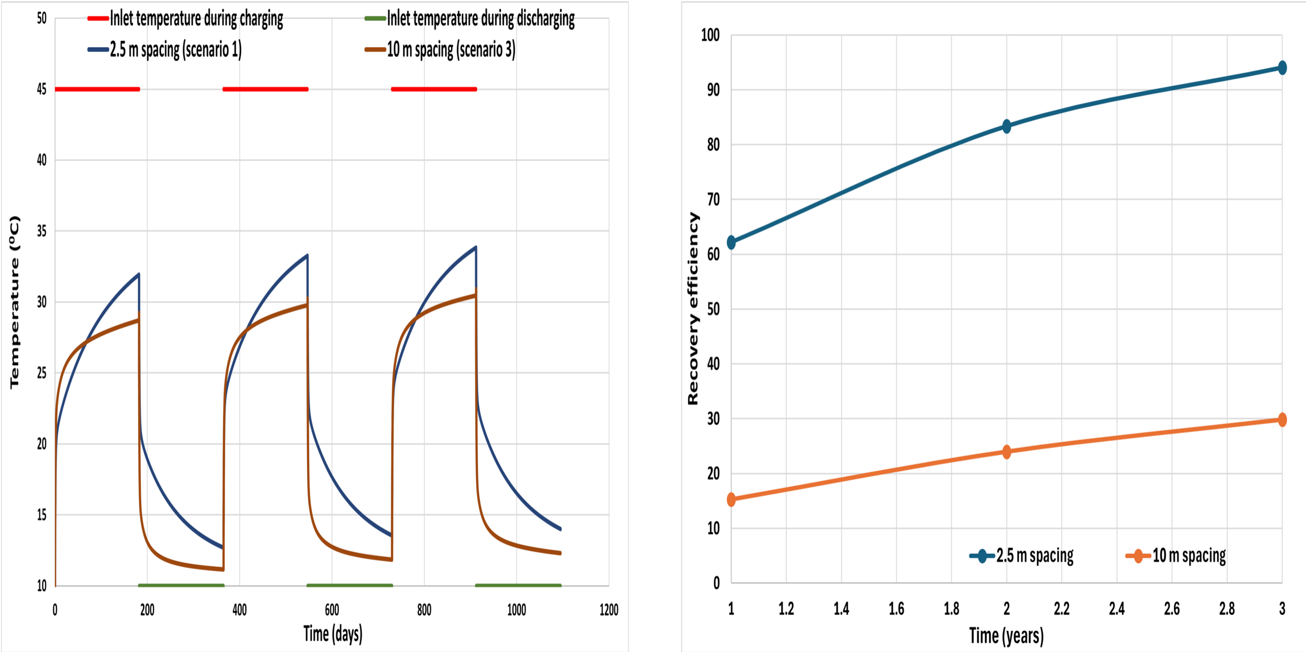

Fig. 11 Temperature profile and recovery efficiency for a 3-year cycle

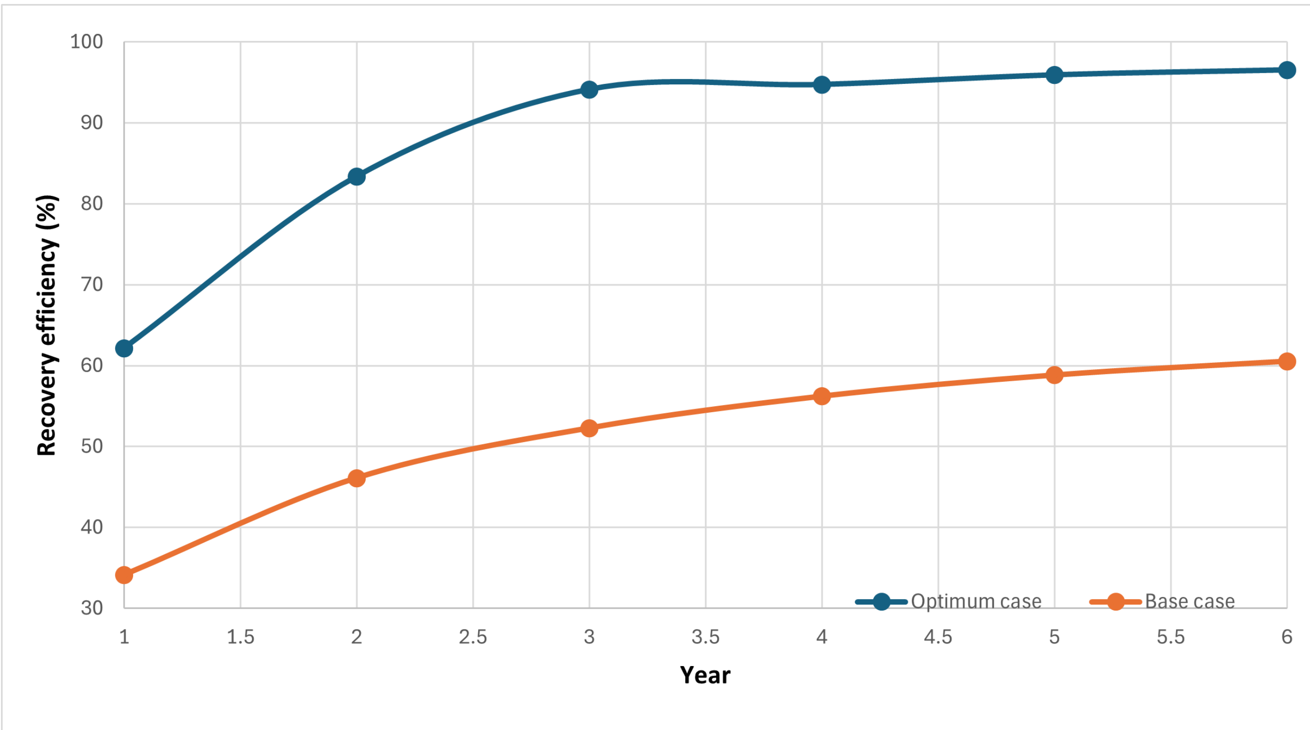

Fig. 12 Recovery efficiency of base case and optimum case